DRFC/CAD EUR-CEA-FC-1578

Self-Sustained Magnetic Islands

J.H. Chatenet, J.F. Luciani,
X. Garbet

June 1996

SELF-SUSTAINED MAGNETIC ISLANDS

J.H. Chatenet, J.F. Luciani
CPHT, Ecole Polytechnique
91128 Palaiseau Cedex, France
X.Garbet
Association Euratom-CEA sur la Fusion Contrôlée
CE Cadarache, 13108 St Paul Lez Durance, France

Abstract

Numerical simulations of a single magnetic island evolution are presented in the regime where the island width is smaller than an ion Larmor radius. It is shown that the island rotation is controlled by particule diffusion due to collisions or a background of microturbulence. More precisely, for vanishing density gradient, the sign of rotation frequency is determined by the off-diagonal diffusion term, i.e., by the coefficient of the temperature gradient in the particle flux. As expected from the theory of a stationary island, there exist cases where linearly stable magnetic perturbation are nonlinearly self-sustained. This situation corresponds to large poloidal beta and temperature gradient. The drive is due to diamagnetic frequency effects. However, this situation is not generic, and islands can also decay. It is found that a magnetic island is self-sustained for a negative off-diagonal diffusion coefficient. This case occurs in a tokamak if the inward particle pinch is due to the temperature gradient.

P.A.C.S.: 52.30.Jb, 52.35.Py, 52.55.Fa, 52.65.+z

I. INTRODUCTION

Diamagnetic effects on magnetic island stability have received considerable attention in the past years. There are essentially two reasons for this. First, many authors [1-5] have claimed that a linearly stable magnetic perturbation could be self-sustained in the nonlinear regime. The latter result requires an island size smaller than an ion Larmor radius and a poloidal beta larger than a threshold value. This threshold scales as the product of the poloidal wavenumber by the island width. This is a possible route towards magnetic turbulence in high beta tokamak discharges. Second, for larger island widths, the diamagnetic effects are usually stabilizing [6-11]. This implies that a magnetic island needs to be triggered [12] before it enters the regime where it grows with a resistive time scale [13], even though the jump of vector potential derivative across the resonant surface is positive (i.e. positive Δ'). The only case where these effects are negligible corresponds to island widths much larger than an ion Larmor radius [14], since the diamagnetic correction to the Rutherford expression goes like the inverse cube of the island width. Also, it has been claimed that microtearing modes can be unstable in tokamak edge plasmas [15].

Theoretical analyses show that the stability of magnetic islands strongly depends on their rotation frequency. In fact, the stability can be reversed if the rotation velocity is not in the right range. This issue about island rotation is related to the problem of locked modes [16,17,10]. Most of the nonlinear studies of magnetic modes rely on the computation of a quasi-stationary state, i.e., they assume the existence of an island which rotates at a given velocity, with possibly slow variations of the island width and pulsation. This excludes fast transients, a point which is crucial for subcritical states, i.e. situations where a magnetic mode is linearly stable and nonlinearly self-sustained. Several mechanisms have been proposed to determine the island rotation frequency : particle diffusion close to the separatrix [1,2], parallel thermal diffusion [4], neoclassical effects modified by the island topology in collisional [10] and low collisionality [11] regimes. The question about which is the dominant process is still open.

The purpose of the present numerical work is to study the full time evolution of an island. Our attention has been focused on subcritical states, corresponding to an island width smaller than an ion Larmor radius, a large poloidal beta and a temperature gradient much larger than the density gradient. The fluid code which has been used accounts for diamagnetic frequency effects and contains the basic ingredients which determine the rotation velocity, apart from trapped electron dynamics (neoclassical effects). It will be shown that self-sustained magnetic islands exist, even when they are linearly stable. There also exists a range of

parameters for which the island shrinks, although it is theoretically predicted to be maintained by diamagnetic currents. This behavior depends crucially on the island rotation frequency. In practice, self-sustainment is found when the density gradient cancels, and for islands drifting in the ion diamagnetic direction. The rotation frequency is determined by particle diffusion. When the density gradient vanishes, it is indeed found that the sign of rotation is determined by the off-diagonal coefficient associated with the temperature gradient in the particle flux. The existence of such a term is suggested by perturbative transport analyses [18]. It is related to the particle pinch in a tokamak, due to the temperature gradient (another possible cause is an effect of the inductive field such as in the Ware pinch). An inward pinch corresponds to a negative off-diagonal term. It turns out that this situation corresponds to an island convection in the ion diamagnetic direction, and self-sustainment in our simulations.

The remainder of the paper is presented as follows. The second section is devoted to the model description. The third part deals with linear stability and summarizes results concerning the stationary nonlinear solutions. The fourth paragraph describes the numerical code which has been used. Numerical results in linear and nonlinear regimes are presented in the same section. A conclusion follows.

II. THE MODEL

A slab geometry is chosen here, which retains the relevant properties of a tokamak equilibrium near a resonant surface. The equilibrium field is given by

$$\mathbf{B} = B_0 \mathbf{e}_z + \nabla A_{eq} \times \mathbf{e}_z \; ; \; A_{eq} = \frac{1}{2}\frac{B_0}{L_s} x^2 \qquad (1)$$

In a tokamak, x is the radial distance to a resonant surface, and L_s is the shear length. This corresponds to an equilibrium current j_{eq} equal to $-B_0/\mu_0 L_s$. The equilibrium density (resp. electron temperature) n_{eq} (resp. T_{eq}) profile is assumed to be linear $n_{eq} = n_0 + n'_{eq} x$ (resp. $T_{eq} = T_0 + T'_{eq} x$). For the sake of simplicity, it is assumed here that there is no equilibrium radial electric field. When a stationary solution is found, the effect of such a field is simply to shift the frequency.

It is now supposed that the plasma is perturbed by an electromagnetic mode, periodic in y, with a period $2\pi/k_y$ (in a tokamak, y is the poloidal direction). The electron response is given by fluid equations [19]. Ignoring third order nonlinearities and electron inertia, the following set of equations is obtained

$$\begin{cases} \partial_t n_e + v_E.\nabla n_e + \nabla_{//}(j_z/e) = D_\perp\left\{\nabla_\perp^2\left(n_e + n_0\frac{eU}{T_0}\right) + \alpha\frac{n_0}{T_0}\nabla_\perp^2 T_e\right\} \\ \partial_t A_z + \frac{T_0}{n_0 e}\nabla_{//}\left(n_e + n_0\frac{eU}{T_0} + \kappa\frac{n_0}{T_0}T_e\right) = -\eta_{//}\left(j_z - j_{eq}\right) \\ \partial_t T_e + v_E.\nabla T_e + \kappa\frac{2T_0}{3n_0}\nabla_{//}(j_z/e) = \frac{2}{3}D_\perp\left\{\alpha\frac{T_0}{n_0}\nabla_\perp^2\left(n_e + n_0\frac{eU}{T_0}\right) + \alpha'\nabla_\perp^2 T_e\right\} \\ \qquad\qquad + \frac{2}{3}\chi_{//}\nabla_{//}^2 T_e \end{cases} \tag{2}$$

where U is the electric potential, $v_E=(e_z x \nabla U)/B_0$ is the electric drift, $\eta_{//}=\eta\nu_c m_e/(2n_0e^2)$ is the resistivity (ν_c is the electron collision frequency, η=1.02, e=-1.602 10^{-19}C is the electron charge), $\chi_{//}$=3/2 χ v_{Te}^2/ν_c is the parallel heat diffusivity ($v_{Te}=\sqrt{2T_e/m_e}$ is the thermal velocity), χ=1.05, κ=1.71, α=-0.5, α'=2.66. The parallel gradient is defined along the perturbed field lines, i.e., $\nabla_{//}F=e_z.(\nabla F x \nabla A_z)/B_{eq}$. The Braginskii diffusion coefficient $D_\perp=1/2\nu_c\rho_e^2$ ($\rho_e=m_e v_{Te}/eB_0$ is the electron Larmor radius) is very small in a tokamak. In fact, the transverse particle and heat transport is controlled by plasma turbulence. We will thus consider $D_\perp$, α and α' as free parameters in the following. Note that an inward particle pinch corresponds to α<0. All quantities are the sum of the equilibrium profile and a perturbation, in particular

$$A_z(x,y) = A_{eq}(x) + \tilde{A}(x,y) \tag{3}$$

Since the island width is supposed to be smaller than an ion Larmor radius, the ion density response is adiabatic, i.e,

$$\frac{\tilde{n}_i}{n_0} = \frac{1}{\tau}\frac{e\tilde{U}}{T_0} \tag{4}$$

where τ is the ratio of the ion temperature to the electron temperature. The self-consistency is ensured by the condition of quasi-neutrality, i.e. $\tilde{n}_i = \tilde{n}_e$, and the Ampère law

$$\nabla_\perp^2 A_z = -\mu_0 j_z \tag{5}$$

It is convenient to introduce the linear mode width $\delta = \sqrt{\left|\nu_c/\omega_{Te}^*\right|}\,(L_s/2L_{Te})\,\rho_e$, where ω_{Te}^* is the diamagnetic frequency associated with the temperature gradient ($\omega_{Te}^* = k_y T_0/eB_0L_{Te}$) and L_{Te} is the electron temperature gradient length. The radial distance is normalized to δ, the coordinate y is normalized to $1/k_y$ and the time is normalized to a diamagnetic time $1/\omega_{Te}^*$ (for convenience, the notations x,y,t will be conserved). The amplitude of the perturbed current is controlled by the parameter

$$\beta_p^* = \frac{4\mu_0 n_0 T_0}{B_0^2}\left(\frac{L_s}{L_{Te}}\right)^2 \tag{6}$$

which scales as a poloidal beta in a tokamak. The following normalized quantities

$$N=\frac{L_{Te}}{\delta}\frac{n_e-n_0}{n_0};J=\sqrt{\left|\frac{\nu_c}{\omega^*_{Te}}\right|}\frac{L_{Te}}{\delta}\frac{\beta^*_p}{4}\frac{j_z}{n_0 e v_{Te}};T=\frac{L_{Te}}{\delta}\frac{T_e-T_0}{T_0}$$
$$U=\frac{L_{Te}}{\delta}\frac{eU}{T_0};A=\sqrt{\left|\frac{\omega^*_{Te}}{\nu_c}\right|}\frac{L_{Te}}{\delta}v_{Te}\frac{eA_z}{T_0} \tag{7}$$

are then governed by the equations

$$\begin{cases}\partial_t N+[U,N]+\frac{4}{\beta^*_p}[J,A]=D_\perp\nabla^2_\perp(N+U+\alpha T)\\ \partial_t A+[N+U+\kappa T,A]=-\frac{4\eta}{\beta^*_p}(J-J_{eq})\\ \partial_t T+[U,T]+\frac{8\kappa}{3\beta^*_p}[J,A]=\frac{2}{3}D_\perp\nabla^2_\perp(\alpha(N+U)+\alpha' T)+\chi[[T,A],A]\\ U=\tau(N-N_{eq})\\ -\nabla^2_\perp A=J\end{cases} \tag{8}$$

With these normalizations, J_{eq}=-1, $N_{eq}=x/\eta_e$ (η_e=dLogT_e/dLogn_e),T_{eq}=x, $A_{eq}=x^2/2$, χ=1.05, η=1.02, κ=1.71, and $D_\perp$ is the diffusion coefficient normalized to $\omega^*_{Te}\delta^2$. The laplacian operator is $\nabla^2_\perp=\partial_{xx}+k_y^2\partial_{yy}$ and the bracket is the usual operator [F,G]=$\partial_x F\partial_y G-\partial_y F\partial_x G$. Defining an energy as

$$E=\frac{1}{2}\int_{-w/2}^{w/2}dx\int_{-\pi}^{\pi}\frac{dy}{2\pi}\left\{\frac{(N+U)^2}{1+\tau}+\frac{4}{\beta^*_p}\left(\nabla_\perp A\right)^2+\frac{3}{2}T^2\right\} \tag{9}$$

the energy balance equation is

$$\begin{aligned}\partial_t E=&-D_\perp\int_{-w/2}^{w/2}dx\int_{-\pi}^{\pi}\frac{dy}{2\pi}\left\{\left[\nabla_\perp(N+U+\alpha T)\right]^2+\left(\alpha'-\alpha^2\right)\left[\nabla_\perp T\right]^2\right\}\\ &-\eta\left(\frac{4}{\beta^*_p}\right)^2\int_{-w/2}^{w/2}dx\int_{-\pi}^{\pi}\frac{dy}{2\pi}J(J-J_{eq})-\frac{3}{2}\chi\int_{-w/2}^{w/2}dx\int_{-\pi}^{\pi}\frac{dy}{2\pi}[T,A]^2+S_{boundary}\end{aligned} \tag{10}$$

where $S_{boundary}$ can be understood as a source term linked to boundary conditions (w is the radial size of the box)

$$S_{boundary}=D_\perp\int_{-\pi}^{\pi}\frac{dy}{2\pi}\left[(N+U)\partial_x(N+U)+\alpha\partial_x((N+U)T)+\alpha' T\partial_x T\right]_{x=-w/2}^{x=w/2} \tag{11}$$

The condition $\alpha'\geq\alpha^2$ has to be fulfilled in order to ensure that the system is dissipative (this is the case for the Braginskii values α=-0.5, α'=2.66).

III. THEORY

1. Linear stability

Assuming a perturbation of the form $\tilde{A}(x,y,t)=\tilde{A}(x)\exp\{i(y-\Omega t)\}$, and neglecting diffusion coefficients, the above system yields the linear current

$$\tilde{J}(x)=\beta_p^*\sigma(x)\tilde{A}(x)$$

$$\sigma(x)=\frac{1}{4}\frac{\Omega(\Omega-1/\eta_e-\kappa)+i\chi x^2(\Omega-1/\eta_e)}{\left(\frac{(1+\tau)x^2}{\Omega+\tau/\eta_e}-i\eta\right)\left(\Omega+i\chi x^2\right)+\kappa\alpha^2\left(\frac{2\kappa}{3}-\frac{\tau}{\Omega+\tau/\eta_e}\right)} \tag{12}$$

As expected, the current is localized within a layer whose width is a few units. Outside this current layer, the solution of the Ampère equation is proportional to $\exp(-|k_y x|)$. If the current is not too large, i.e, for moderate β_p^*, the variation of the vector potential in the layer is weak and the constant A approximation holds. The matching of the slopes give the following constraint

$$2|k_y|=\beta_p^*\int_{-\infty}^{+\infty}dx\sigma(x) \tag{13}$$

Two type of modes are potentially unstable:

i) Small scale modes, which are similar to η_e modes [20-22]. Their stability is controlled by η_e . This property can be recovered with a Wentzel-Kramers-Brillouin analysis. Let us assume that $\tilde{A}(x)$ behaves as $\exp\left(i\int k(x)dx\right)$. The Ampère equation then reduces to $k(x)^2=\beta_p^*\sigma(x)$. It can be verified from (12) that if τ is finite, an unstable solution exists at large values of $k(x)$ if $\eta_e>\eta_{ec}$, where $\eta_{ec}=2\kappa/3+\chi/\kappa$ (≈ 1.75). This solution is radially localized close to $\pm(\eta\gamma/\kappa)^{1/2}/(\eta_e-\eta_{ec})^{1/2}$, where γ is the growth rate. However, it is expected that these small scale modes are stabilized by diffusion processes. In the case where the ion temperature is zero ($\tau=0$, corresponding to a vanishing perturbed electric potential), there is no instability. This is precisely the situation which has been chosen in the numerical analysis. This analysis shows indeed that the modes are linearly stable. For finite τ, the same analysis shows unstable η_e modes provided that the perpendicular diffusion coefficients are small.

ii) Collisional microtearing modes [23,24]. These modes can be unstable above a β_p^* threshold. The main destabilizing current is the contribution far from the resonant surface. In this region, the current decreases as $1/x^2$

$$\tilde{J}(x)=\frac{\beta_p^*}{4(1+\tau)x^2}(\Omega-1/\eta_e)(\Omega+\tau/\eta_e)\tilde{A}(x) \tag{14}$$

It is destabilizing if positive, i.e., if $\Omega>1/\eta_e$ or $\Omega<-\tau/\eta_e$ and may drive a microtearing mode. However, the sign of the current usually changes when |x| decreases. This leads to small values of the integral in Eq.(13) and therefore to a high β_p^* threshold. An analytic study of Eqs. (12) and (13) within the frame of the constant A approximation shows that no marginal mode, and therefore no unstable mode, can be found, whatever β_p^* (see Appendix). The numerical analysis, which allows to relax the constant A approximation, confirms this result (see section IV.2). This result holds when the diffusion coefficients are finite. This is similar to the previous observation along which there is no instability in the fluid regime when the layer width is larger than an ion Larmor radius [25] (we remind the reader that the present work assumes the opposite limit). However, this disagrees with the kinetic result, which shows that there exists a finite β_p^* threshold in both regimes where the linear width is larger [26] or smaller [27] than an ion Larmor radius. This point was already noticed by Hassam [28], who proposed to introduce a time-dependent thermal force in the Braginskii mechanical equation. An instability is then recovered [25,29]. However, since the collisional kinetic analysis shows that the threshold is large in the regime we investigate, we will not modify the Braginskii system. Our starting point is therefore a linearly stable situation. It is expected that in the nonlinear regime, the shape of the current is mainly given by the above expression because of the radial cut-off introduced by the island itself (assuming that there is no diamagnetic current inside the island). An illustration is given in the following.

2 Nonlinear stationary solution

Let us suppose now that there exists a nonlinear solution such that $\tilde{A}(x,y,t)=2\tilde{A}(x)\cos(y-\Omega t)$, i.e., corresponding to a total vector potential

$$A(x,y,t)=\frac{x^2}{2}+2\tilde{A}(x)\cos(y-\Omega t) \qquad (15)$$

It is supposed that $\tilde{A}$ varies smoothly in the x direction (constant A approximation). Thus, the normalized island half-width δ_I equals $\sqrt{8\tilde{A}(0)}$. The calculation of the nonlinear solution has been given in details elsewhere [1, 4, 9] and will only be summarized here. The calculation is greatly simplified if the radial coordinate is normalized to δ_I. Introducing $\rho=x/\delta_I$, $u=y-\Omega t$ and $a=\rho^2/2+\cos(u)/4$, and writing all quantities as functions of a and u, the system (8) can be rewritten

$$\begin{cases} [I,a]+\dfrac{1}{\delta_I^2}[V,M]=\dfrac{D_\perp}{\delta_I^3}\nabla_\perp^2(M+\alpha T) \\ [M+\kappa T,a]=-\dfrac{\eta}{\delta_I}\left(I-I_{eq}\right) \\ \dfrac{2\kappa}{3}[I,a]+\dfrac{1}{\delta_I^2}[V,T]=\dfrac{2}{3}\dfrac{D_\perp}{\delta_I^3}\nabla_\perp^2(\alpha M+\alpha' T)+\chi\delta_I[[T,a],a] \\ V(1+\tau)=\tau M-(\tau/\eta_e+\Omega)\delta_I\rho \\ \left|k_y\delta_I\right|=\beta_p^*\int d\rho\dfrac{du}{2\pi}\cos(u)I \end{cases} \tag{16}$$

where $V=U-\Omega x$, $M= N+U-\Omega x$ and $I=4/\beta_p^*$ J. The brackets now involve derivatives with respect to ρ and u. Two small parameters can be identified. First, the ratio of the diffusive time to the parallel transit time, given by $D_\perp/\delta_I^3$. This parameter characterizes diffusive processes. The second parameter characterizes diamagnetic effects and is proportional to the diamagnetic frequency divided by the parallel transit time, i.e., is given by $1/\delta_I$ with the present conventions. We assume for simplicity that these two small parameters are of the same order. The analysis with two small parameters can be found in the references previously quoted. The quantities M, I, T, and V are then written as series, e.g., $M=M_0O(\delta_I)+M_1+M_2O(1/\delta_I)+...$ It is easily found that M_0, I_0, T_0, T_1 are flux functions (do not depend on $u=y-\Omega t$). Note that V_0 is not a flux function and is given by

$$V_0(1+\tau)=\tau M_0-(\tau/\eta_e+\Omega)\delta_I\rho \tag{17}$$

The following order can be written

$$\begin{cases} \left[I_1+\dfrac{1}{\delta_I^2}\dfrac{dM_0}{da}V_0,a\right]=\dfrac{D_\perp}{\delta_I^3}\nabla_\perp^2(M_0+\alpha T_0) \\ [M_1+\kappa T_1,a]=-\dfrac{\eta}{\delta_I}I_0 \\ \left[\dfrac{2\kappa}{3}I_1+\dfrac{1}{\delta_I^2}\dfrac{dT_0}{da}V_0,a\right]=\dfrac{2}{3}\dfrac{D_\perp}{\delta_I^3}\nabla_\perp^2(\alpha M_0+\alpha' T_0)+\chi\delta_I[[T_2,a],a] \end{cases} \tag{18}$$

Defining a flux average as

$$\langle F\rangle=\frac{\oint\dfrac{du}{2\pi}\dfrac{F(a,u)}{G(a,u)}}{\oint\dfrac{du}{2\pi}\dfrac{1}{G(a,u)}};G(a,u)=\left|\frac{\partial a}{\partial\rho}\right|(a,u) \tag{19}$$

the flux averages of the above equations lead to

$$\left\langle\nabla_\perp^2M_0\right\rangle=0,\left\langle\nabla_\perp^2T_0\right\rangle=0,I_0=0 \tag{20}$$

which express particle and heat flux conservation across the island. Imposing that M_0 and T_0 approach the equilibrium profiles far from the island, the solutions of the above equation are easily found

$$\begin{cases} \dfrac{dM_0(a)}{da} = \delta_I (1/\eta_e - \Omega)\ sg(\rho)\ Q(a) \\ \dfrac{dT_0(a)}{da} = \delta_I\ sg(\rho)\ Q(a) \end{cases} \tag{21}$$

where

$$Q(a) = \begin{cases} 0 & \text{inside the island} \\ \left[\oint \dfrac{du}{2\pi} G(a,u) \right]^{-1} & \text{outside the island} \end{cases}$$

and $sg(\rho)$ is the sign of ρ. Apart from the equilibrium current, the current I_I is the sum of a current I_{diff} due to particle diffusion and a "diamagnetic current" I_{dia}. The first one is determined by the following equation

$$\frac{\partial I_{diff}}{\partial u} = -\frac{D_\perp}{\delta_I^2}(1/\eta_e + \alpha - \Omega)\frac{\partial}{\partial a}[GQ] \tag{22}$$

I_{diff} is an even function of ρ and decreases as $1/\rho^4$. It is in quadrature of phase with the island and therefore induces a rotation. In a stationary regime, no current in quadrature of phase is allowed and the rotation frequency is given by

$$\Omega = 1/\eta_e + \alpha \tag{23}$$

The diamagnetic current I_{dia} is given by

$$I_{dia} = -\frac{1}{\delta_I^2}\frac{dM_0}{da}\left(V_0 - \langle V_0 \rangle\right) \tag{24}$$

where the constraint $\langle I_{dia} \rangle = 0$ has been used (this constraint is provided by $O(1/\delta_I)$ equations). The diamagnetic current $J_{dia} = \beta_p^*/4\ I_{dia}$ is in phase with the vector potential and can be written

$$J_{dia} = \frac{\beta_p^*}{4(1+\tau)}(\Omega - 1/\eta_e)(\Omega + \tau/\eta_e)Q(a)\left(\langle|\rho|\rangle - |\rho|\right) \tag{25}$$

As expected, the structure of this current is similar to the linear one far from the island. They are asymptotically identical when ρ approaches infinity (in particular, both are even functions of ρ and decrease as $1/\rho^2$). The matching condition within the frame of the constant A approximation yields the condition for a growing island

$$\begin{aligned} &\frac{\beta_p^*}{|k_y|\delta_I(1+\tau)}(\Omega - 1/\eta_e)(\Omega + \tau/\eta_e) > \frac{1}{C} \\ &C = 2\int_{1/4}^{+\infty} da\, Q(a)\langle|\rho|\rangle\left[\int_{-\pi}^{+\pi}\frac{du}{2\pi}\frac{\cos(u)}{G(a,u)}\right] = 0.4 \end{aligned} \tag{26}$$

Diamagnetic frequency effects are therefore destabilizing if $\Omega>1/\eta_e$ or $\Omega<-\tau/\eta_e$. Using the dispersion relation Eq.(23), the latter condition requires that $\alpha>0$ or $\alpha<-(1+\tau)/\eta_e$. For flat density profiles, i.e. large values of η_e, this condition is always fulfilled.

It must be emphasized that the calculation of the island rotation frequency is still an open question. Several mechanisms have been proposed in the literature: neoclassical effects in collisional [10] and collisionless [11] regimes, thermal parallel diffusion [4] and particle diffusion [1,2]. Only the latter two effects can be tested here. In the work of Smolyakov, the diffusion coefficients are not included in the calculation of the rotation frequency, although it is assumed that a diffusion process determines the density and temperature profiles. The above calculation shows that the temperature field T_2 is in quadrature of phase with the potential vector and is given by the relation

$$\chi G(a,u)\frac{\partial T_2}{\partial u}=\frac{sg(\rho)}{\delta_I}\left(\frac{1}{\eta_e}-\frac{3}{2\kappa}-\Omega\right)\left(\frac{\tau}{\eta_e}+\Omega\right)\frac{2\kappa}{3(1+\tau)}Q(a)\left(\langle|\rho|\rangle-|\rho|\right) \qquad (27)$$

which is similar to the expression given by Smolyakov [4]. This behavior leads to a finite dissipation term in the energy balance equation Eq.(10). Without any diffusion, this is the only source of dissipation (the linear ohmic term cancels because the flux average of the diamagnetic current is zero and the quadratic term is small and compensated by the ohmic heating term which has been neglected here) and has to cancel in a stationary regime. This constraint provides either the dispersion relation $\Omega=-\tau/\eta_e$, which cancels the diamagnetic current, or $\Omega=1/\eta_e-3/(2\kappa)$, which leads to an instability for large enough values of η_e, $\eta_e>2\kappa(1+\tau)/3$ (the value given by Smolyakov is slightly different due to a different definition of the energy). In the latter case the island rotates in the ion diamagnetic direction. A competition is expected between this effect and the diffusion drive described above. With the present ordering, it is expected that diffusion effects will be dominant.

IV NUMERICAL RESULTS

1. Code description

We study the full time evolution of one magnetic island. The time integration of Eqs.(8) uses a fourth-order explicit Runge-Kutta scheme with adaptative time step. The derivatives in the radial direction are evaluated by finite differences, while derivatives in the y-direction are computed via Fourier transform. The gradients are set through boundary conditions at $x=\pm w/2$,

where w is the box width. More precisely, $A(\pm w/2,y)=w^2/8$, $U(\pm w/2,y)=0$, $N(x,y)=\pm w/2\eta_e$, and $T(\pm w/2,y)=\pm w/2$. At t=0, the vector potential is set to

$$A(x,y,t=0)=x^2/2+\tilde{A}_0(x-w/2)(x+w/2)\cos(y)$$

where $\tilde{A}_0$ equals a few times 0.01. Other quantities are initialized to their equilibrium values $U(x,y)=0$, $N(x,y)=x/\eta_e$, and $T(x,y)=x$. To avoid oscillations on a grid scale due to the convection, hyperdiffusion terms have been added, following the usual procedure (see for instance Guzdar et al.[30]). For dealiasing, we set to zero the upper third part of the Fourier components at each time step . In order to show the long time evolution of the island, we use long runs of 10^5 to $5\ 10^5$ time steps.

To maintain satisfactory numerical stability, the time step is limited to less than 10^{-3}. Thus we limit the study to a moderate resolution: all calculations are done with 100 grid points in x (w=100) and 32 harmonics in y. The width of the diffusive layer close to the separatrix (at the O point) is of the order of $(D_\perp/\chi)^{1/2}$. On the other hand, the diffusion coefficient $D_\perp$ has to be low enough, typically of order unity. This leads to a diffusive layer which is too small when compared to the grid mesh. To increase this size, the parallel diffusivity has been decreased by a factor 100 ($\chi = 1.05\ 10^{-2}$). This operation does not change the basic ordering.

The sign of rotation of an island is deduced from the time evolution of the vector potential at x=0 and 3 different values of y : 0, $\pi/2$, and π. If A(x=0,y=0) closely precedes the two other signals, the rotation is positive, whereas a leading $A(x=0,y=\pi/2)$ corresponds to a negative rotation. The value of the rotation frequency is deduced from the elapsed time between two minima of A(x=0,y=0). The temperature map allows to visualize the island topology at any time. This topology can then be compared with the maps for density, current and flux.

2. Linear regime

To study the linear phase, the code has been used with small initial amplitudes. It is assumed that the regime is linear when the initial island width is of the same order as the linear width. The results have been cross-checked with a code solving a linearized version of Eqs. (8). The latter code is faster since it uses an implicit scheme. Without diffusion ($D_\perp = 0$), and for a finite ratio of the ion to electron temperature τ, we find an instability above a η_c threshold. The spatial structure of this unstable mode is close to the structure of the η_e modes described in section III.1. In particular, spikes in the vector potential grow up at the poles of the conductivity. The observed value of the threshold is in good agreement with the theoretical expectation, i.e. $\eta_e=1.7$. For $\tau=0$, the mode is always stable, as expected. An example is given

shows a mode decay. The parameters correspond to the non-linear case where a self-sustained island is found.

3. Nonlinear regime

In the nonlinear regime, a simulation generally begins with a transient phase where density and temperature profiles rearrange themselves to form an island. This is followed by a slower evolution of the island. In what follows, we have chosen k_y=0.025, and τ=0 (in this case, the perturbed potential vanishes). In practice, the results are rather insensitive to the values of $D_\perp$ (0.6 or 3), β_p^* (10 or 20) , and $\tilde{A}_0$ (ranging between 0.04 and 0.08). These values of $D_\perp$ correspond to a typical background of turbulence in a tokamak, whereas β_p^* is larger than the actual value in a tokamak. Thus, two parameters play an important role: α and η_e. In order to simplify the comparison with the results of the section III, we have chosen $\eta_e=\infty$. In this case, the island is expected to be self-sustained whatever the sign of α, since the condition (26) is always fulfilled except for small values of α. Several cases have been simulated with α ranging from -1 to +1 (we remind the reader that Braginskii equations correspond to α=-0.5 and that α^2 has to be smaller than α'=2.66). In practice, two types of situations have been encountered, depending on the value of α.

For α =-0.5, 0.5, and 1, we observe a damping of the island (Fig.2). The rotation frequency Ω, measured with the phase shift of the vector potential at three different positions in the y direction, has the sign of α. The damped island shrinks into the O-point (Fig.3a and 3b), surrounded by a current sheath (Fig.4a). The location of the shrinking O-point is marked by a negative current spike (Fig.4b). The X-point degenerates in a long plateau.

For α=−1, the mode amplitude increases, as shown in Fig.5. At any time, the island retains its shape during the convection. The plateau of temperature in the island remains clearly visible (see Fig.6). Out of the island the N-profile, which we initially set to zero ($\eta_e=\infty$), shows a steep gradient in the vicinity of x=0 with a sign opposite of that of the temperature gradient (Fig.7). This can be understood from the model of section III.2: the function N-Ωx has to be a flux function, which vanishes inside the island. Since the potential vanishes (τ=0), this means that $\Omega \approx dN/dx$ inside the island. The current profile shown on Fig.8 exhibits a dip near the boundary of the island visible on the section passing through the O-point. From this we can infer that diamagnetism effectively plays a significant role in the mechanism leading to self-sustained islands. It is reminded here that this situation is linearly stable, as shown in Fig.1. In summary, this case corresponds to the picture described in section III.2.

4. Discussion

The above simulations yield some interesting indications on the physics of the island rotation and stability. The island rotation appears to be conditioned by the perpendicular diffusion. In the case where $D_\perp$=0, there is no rotation, at least on the time scale we are looking at. Rotation frequency, as a function of α, is plotted in Fig. 9. Concerning the dispersion relation given in section III-2, Eq.(23), i.e., $\Omega = 1/\eta_e + \alpha$, the trend is respected, but the slope is lower by a factor two. As written before, the initial amplitude $\tilde{A}_0$, beta β_p^* and perpendicular diffusion coefficient $D_\perp$ have little effect on the actual value of the rotation Ω. The results concerning the stability are more surprising. The case corresponding to α=-1 follows the theoretical model, in particular the current outside the island corresponds to the expectation for the diamagnetic current. Thus, this is an example of a magnetic mode which is linearly stable and nonlinearly self-sustained. The reason why the island shrinks for α=-0.5,0.5 and 1 is not well understood. The island enters very rapidly in a regime where the constant A approximation is no longer correct and the details of this evolution are difficult to describe precisely. In particular, the perturbed vector potential strongly departs from an harmonic shape (i.e. proportional to cos(y-Ωt)), which is assumed in analytical calculations. It seems that the thermal layer surrounding the island diffuses towards the O point, leaving a plateau where the perturbed flux is completely expelled, and concentrating the flux around the same point, in a current ribbon that shrinks and vanishes. This mechanism seems to overcome the diamagnetic current effect described in section III.2, whereas the predicted convective velocity is correct in trend. This behavior remains to be explained in detail. It seems to be generic when the parameter η_c is finite. This suggests that nonlinear analytic calculations should be taken with some care, at least in the case where the island width is smaller than an ion Larmor radius. The case where the island width is larger than an ion Larmor radius remains to be studied.

V CONCLUSION

The time evolution of an island whose width is smaller than an ion Larmor radius has been simulated in the fluid regime. It has been found that the rotation of an island is controlled by the perpendicular diffusion owing to collisions or to a small scale turbulence. The rotation frequency is in rough agreement with the theory for a single stationary island. In particular, the coefficient of the temperature gradient in the dispersion relation is given by the cross term in the matrix diffusion equation, i.e., the coefficient of the temperature gradient term in the particle flux. Cases have been found where a magnetic island is self-sustained whereas any magnetic

perturbation is stable in the linear regime. The destabilizing current is likely due to diamagnetic frequency effects. This is again in agreement with theory. However, this situation is not generic. In many cases, the island shrinks, even for a range of parameters where it is predicted to be self-sustained. This indicates that the standard theory should be taken with care in the sub-gyroradius regime. The reason why islands shrink in situations where self-sustainment was expected is yet to be explained. Interestingly, the regime where self-sustained islands are observed corresponds to a negative off-diagonal coefficient in the particle flux. This is a case in a tokamak where a negative temperature gradient induces a particle inward pinch. This would agree with the actual situation, where an inward pinch is observed, although it is not yet clear whether this pinch is due to the temperature gradient or another source such as the inductive field. It must also be emphasized that a microtearing turbulence, i.e. a situation with many overlapping islands, corresponds to a positive off-diagonal coefficient [1,2]. This case is found to be stable here. The present study therefore applies to an isolated tearing mode, surrounded by a microturbulence which is not a microtearing turbulence.

ACKNOWLEDGEMENTS

The authors would like to thank M. Zabiégo for fruitful discussions. One of the authors (J.H.C.) would like to acknowledge financial supports from the Direction de la Recherche et de la Technologie and the Commissariat à l'Energie Atomique. The calculations have been performed on the computing facilities of the Institut du Développement et des Ressources en Informatique Scientifique, Centre National de la Recherche Scientifique.

FIGURES

Figure 1 : Amplitude of the vector potential as a function of time at x=0 and y=0 (solid curve), $y=\pi/2$ (dashed curve) and $y=\pi$ (broken curve). Parameters are $\tilde{A}_0=0.0005$, $k_y=0.025$, $\tau=0$, $D_\perp=0.6$, $\beta_p^*=10$, $\eta_e=\infty$ and $\alpha=-1$. The rotation frequency is $\Omega = + 1.7$.

Figure 2 : Amplitude of the vector potential as a function of time at x=0 and y=0 (solid curve), $y=\pi/2$ (dashed curve) and $y=\pi$ (broken curve). Parameters are $\tilde{A}_0=0.04$, $k_y=0.025$, $\tau=0$, $D_\perp=0.6$, $\beta_p^*=10$, $\eta_c=\infty$ and $\alpha=1$. The rotation frequency is $\Omega = + 0.2$.

Figure 3 : Temperature map T(x,y) at times t=199 (a) and t=399 (b). Same parameters as in Fig.2.

Figure 4 : In (a), current density J(x,y) at t=399. The negative spike corresponds to the location of the O-point. In (b), radial profile of the current density through the O-point (solid curve) and X-point (broken curve). Same parameters as in Fig.2.

Figure 5 : Amplitude of the vector potential as a function of time at x=0, and y=0 (solid curve), $y=\pi/2$ (dashed curve) and $y=\pi$ (broken curve). Parameters are $\tilde{A}_0=0.04$, $k_y=0.025$, $\tau=0$, $D_\perp=0.6$, $\beta_p^*=10$, $\eta_c=\infty$ and $\alpha=-1$. The rotation frequency is $\Omega=-0.5$.

Figure 6 : Temperature map T(x,y) at t=400.5. Same parameters as in Fig.5.

Figure 7 : Radial profiles of the density N through the O-point (solid curve) and at the X-point (broken curve). Same parameters as in Fig.5.

Figure 8 : Radial profiles of the current J through the O-point (solid curve) and X-point (broken curve). Same parameters as in Fig.5.

Figure 9 : $\Omega - 1/\eta_e$ as a function of α. The cases where the island is damped are indicated by triangles ($\beta_p^*=10$: open triangles, $\beta_p^*=20$: closed triangles). The self-sustained cases are marked by squares ($\beta_p^*=10$: open squares, $\beta_p^*=20$: closed square). A linear fit of these points (solid curve) and the theoretical relation $\Omega - 1/\eta_e = \alpha$ (broken curve) are also shown.

REFERENCES

[1] A. Samain, Plasma Phys. Contr. Fusion **26**, 731 (1984).

[2] P.H. Rebut and M. Hugon, Plasma Phys. Contr. Fusion **33**, 1085 (1991).

[3] B.B. Kadomtsev, Nucl. Fus. **31**, 1301 (1991).

[4] A. I. Smolyakov, Plasma Phys. Contr. Fusion **35**, 657 (1993).

[5] J.W. Connor and H.R. Wilson, Phys. Plasmas **2**, 4575 (1995).

[6] A. I. Smolyakov, Sov. J. Plasma Phys. **15**, 667 (1989).

[7] B.D. Scott and A.B. Hassam, Phys. Fluids **30**, 90 (1987).

[8] R. Fitzpatrick and T.C. Hender, Phys. Fluids **B3**, 644 (1991).

[9] M. Zabiégo and X. Garbet, Phys. Plasmas **1**, 1890 (1994).

[10] A.I. Smolyakov, A. Hirose, E. Lazzaro, G.B. Re, and J.D. Callen, Phys. Plasmas **2**,1581 (1995).

[11] H.R. Wilson, J.W. Connor, R.J. Hastie, C.C Hegna, Phys. Plasmas **3**, 248 (1995).

[12] M. Zabiégo and J.D. Callen, submitted to Nucl. Fusion.

[13] P.H. Rutherford, Phys. Fluids **16**, 1903 (1973).

[14] M.A. Dubois, P. Ghendrih, B. Pégourié, R. Sabot, A. Samain, M. Zabiégo, Plasma Phys. and Contr. Fusion **36**, B55 (1994).

[15] Y.T. Lau, Nucl. Fus. **30**, 934 (1990).

[16] T.H. Jensen, A.W. Leonard, and A.W. Hyatt, Phys. Fluids B5, 1239 (1993).

[17] R. Fitzpatrick, R.J. Hastie, T.J. Martin, C.M. Roach, Nucl. Fusion **33**, 1533 (1993).

[18] G.M.D. Hogeweij, J. O'Rourke, A.C.C. Sips, Plasma Phys. and Contr. Fusion, **33**, 189 (1991).

[19] S.I. Braginskii, in *Reviews of Plasma Physics*, edited by M.A. Leontovitch (Consultants Bureau, New York, 1965), Vol.I, p.205

[20] Y.C. Lee, J.Q. Dong, P.N. Guzdar, C.S. Liu, Phys. Fluids **30**, 1331 (1987).

[21] J.F. Drake, P.N. Guzdar, A.B. Hassam, Phys. Rev. Lett. **61**, 2205 (1988).

[22] A. Hirose, Phys. Fluids B **2**, 850 (1990).

[23] R.D. Hazeltine, D. Dobrott, T.S. Wang, Phys. Fluids **18**, 1778 (1975).

[24] J.F. Drake and Y.C. Lee, Phys. Fluids **20**, 1341 (1977).

[25] J.F. Drake, T.M. Antonsen, A.B. Hassam and N.T. Gladd, Phys. Fluids **26**, 2509 (1983).

[26] J.F. Drake, N.T. Gladd, C.S. Liu, and C.L. Chang, Phys. Rev. Lett. **44**, 994 (1980).

[27] X. Garbet, F. Mourgues. and A. Samain, Plasma Phys. Contr. Fusion **32**, 917 (1990).

[28]A.B. Hassam, Phys. Fluids **23**, 80 (1980).

[29] G.G. Craddock and P.W. Terry, Phys. Fluids B **3**, 3286 (1991).

[30] P.N. Guzdar, J.F. Drake, D. McCarthy, A.B. Hassam, C.S. Liu, Phys. Fluids B **5**, 3712 (1993).

APPENDIX

Linear analysis within the frame of the constant A approximation.

Using Eqs (12) and (13), the matching condition within the frame of the constant A approximation is

$$\frac{\beta_p^*}{8|k_y|}\frac{(\Omega-1/\eta_e)(\Omega+\tau/\eta_e)}{(1+\tau)}=\frac{1}{I(\Omega)} \tag{A1}$$

where

$$I(\Omega)=\int_{-\infty}^{+\infty}dx\,\bar{\sigma}(x)$$
$$\bar{\sigma}(x)=\frac{x^2-ia(\Omega)}{x^4-ib(\Omega)x^2-c(\Omega)} \tag{A2}$$

and

$$a(\Omega)=\frac{\Omega(\Omega-1/\eta_e-\kappa)}{\chi(\Omega-1/\eta_e)}$$
$$b(\Omega)=\frac{\eta}{(1+\tau)}(\Omega+\tau/\eta_e)+\frac{\Omega}{\chi}+\frac{\kappa}{\chi(1+\tau)}\left(\frac{2\kappa}{3}(\Omega+\tau/\eta_e)-\tau\right) \tag{A3}$$
$$c(\Omega)=\frac{\eta\Omega}{\chi(1+\tau)}(\Omega+\tau/\eta_e)$$

Here, we look for marginal modes, i.e., modes for which the frequency Ω is real. The integral $I(\Omega)$ can be evaluated by the calculus of residues. The function $\bar{\sigma}(x)$ usually exhibits 2 pairs of opposite complex poles. We will note x_+ and x_- the two poles in the upper half of the complex plane. The calculation yields

$$I=\frac{i\pi}{x_++x_-}\left(1+i\frac{a}{x_+x_-}\right) \tag{A4}$$

The product $(x_+x_-)^2$ equals -c. Two cases have to be considered:

1) $c(\Omega)>0$ ($\Omega<-\tau/\eta_e$ or $\Omega>0$)

In this case, x_+x_- is a pure imaginary number. An analysis of poles shows that the phase of x_++x_- is $\pm\pi/4$. This means that $I(\Omega)$ cannot be a real, which implies that Eq.(A1) cannot be satisfied.

2) $c(\Omega)<0$ ($-\tau/\eta_e<\Omega<0$)

The poles of $\bar{\sigma}(x)$ are given by

$$x_+ = e^{i\pi/4}\rho_+ \quad ; \quad \rho_+ = \left(\frac{b}{2}+\sqrt{\frac{b^2}{4}-c}\right)^{1/2}$$

$$x_- = e^{3i\pi/4}\rho_- \quad ; \quad \rho_- = \left(-\frac{b}{2}+\sqrt{\frac{b^2}{4}-c}\right)^{1/2} \tag{A5}$$

$$x_+x_- = -\sqrt{-c}$$

Since $I(\Omega)$ has to be real, one finds the relations

$$I = \frac{\pi}{\sqrt{2}\left(\rho_+^2+\rho_-^2\right)}\frac{\left(\rho_+-\rho_-\right)^2+\left(\rho_++\rho_-\right)^2}{\rho_++\rho_-} \tag{A6}$$

$$\frac{a}{\sqrt{-c}} = -\frac{\rho_+-\rho_-}{\rho_++\rho_-} \tag{A7}$$

The relation (A6) implies that $I(\Omega)$ is positive. However, a positive $I(\Omega)$ is not compatible with the matching condition (A1), which indicates that if $-\tau/\eta_c<\Omega<0$ ($c<0$), $I(\Omega)$ has to be negative. Again, there is no solution in this case.

In summary, the above study shows that in all cases, there is no marginal solution within the frame of the constant A approximation.

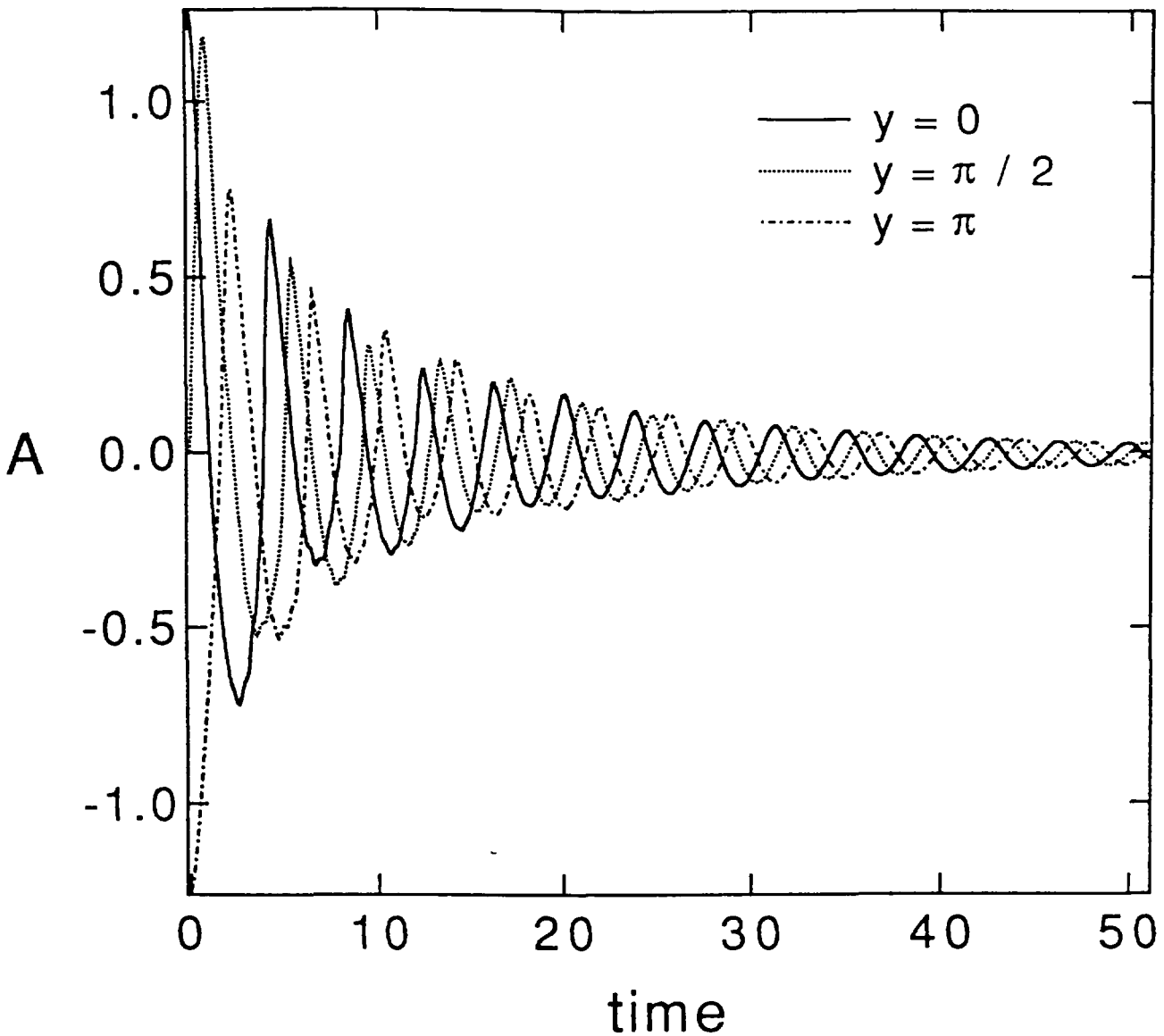

Fig. 1

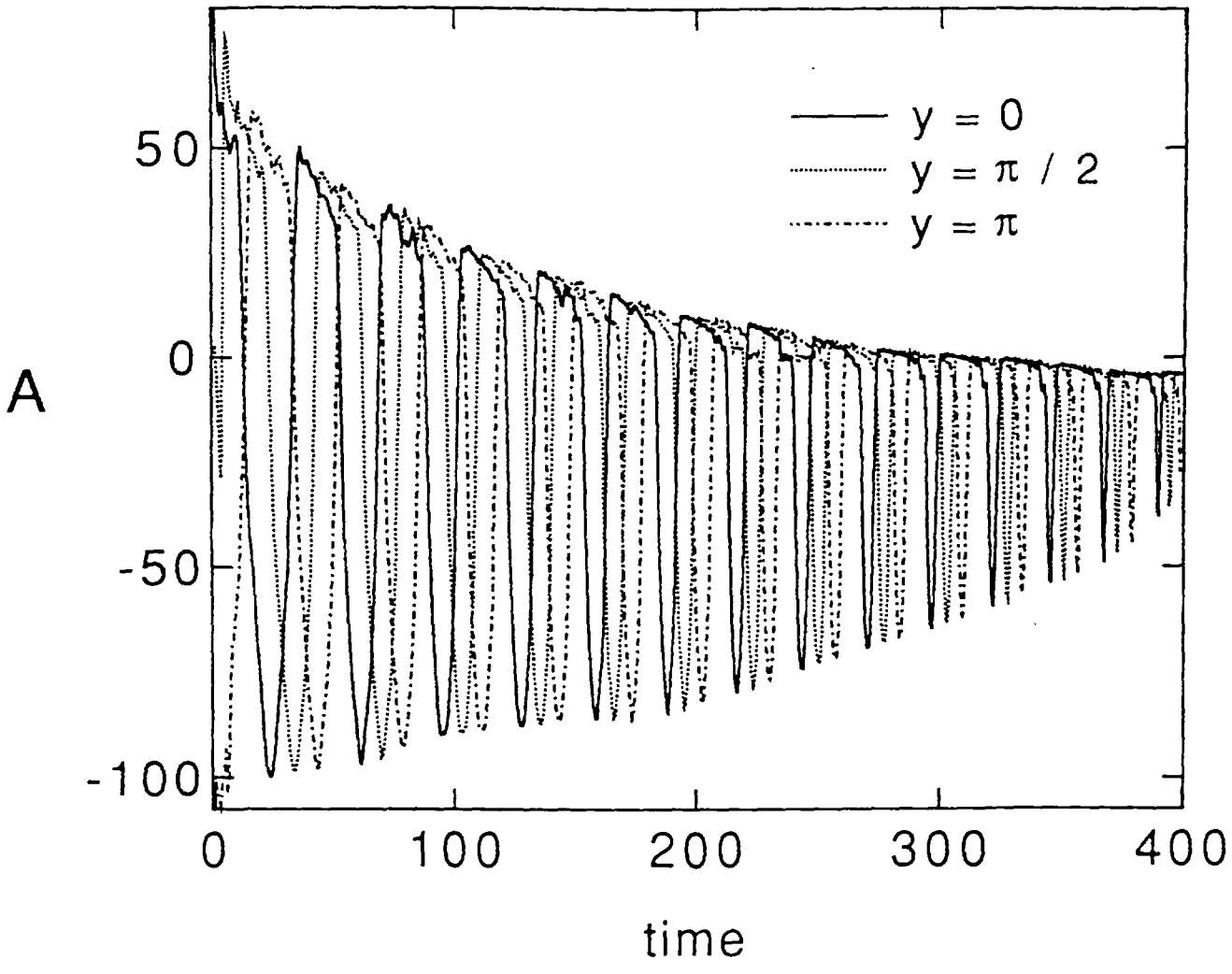

Fig. 2

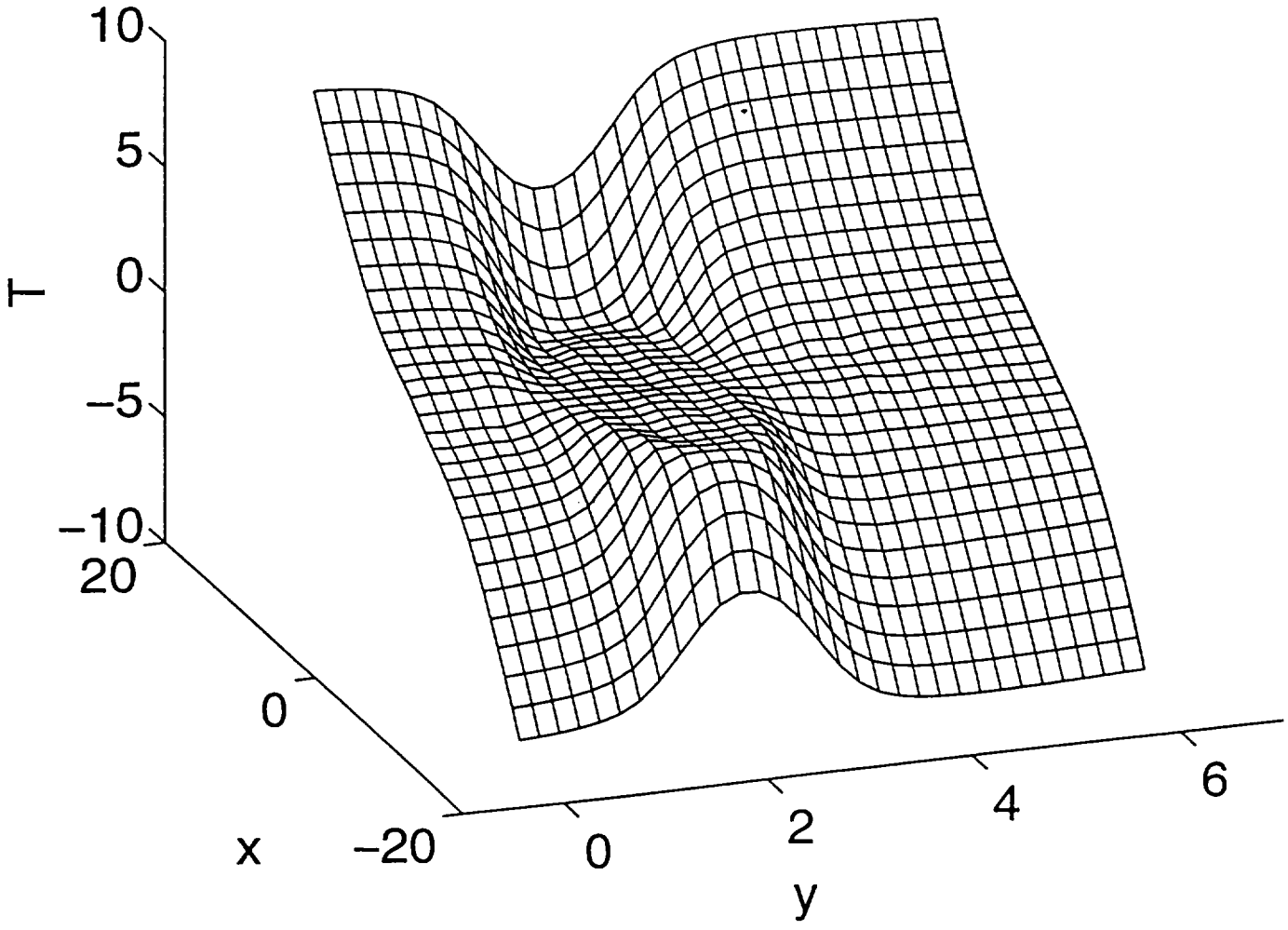

Fig. 3a

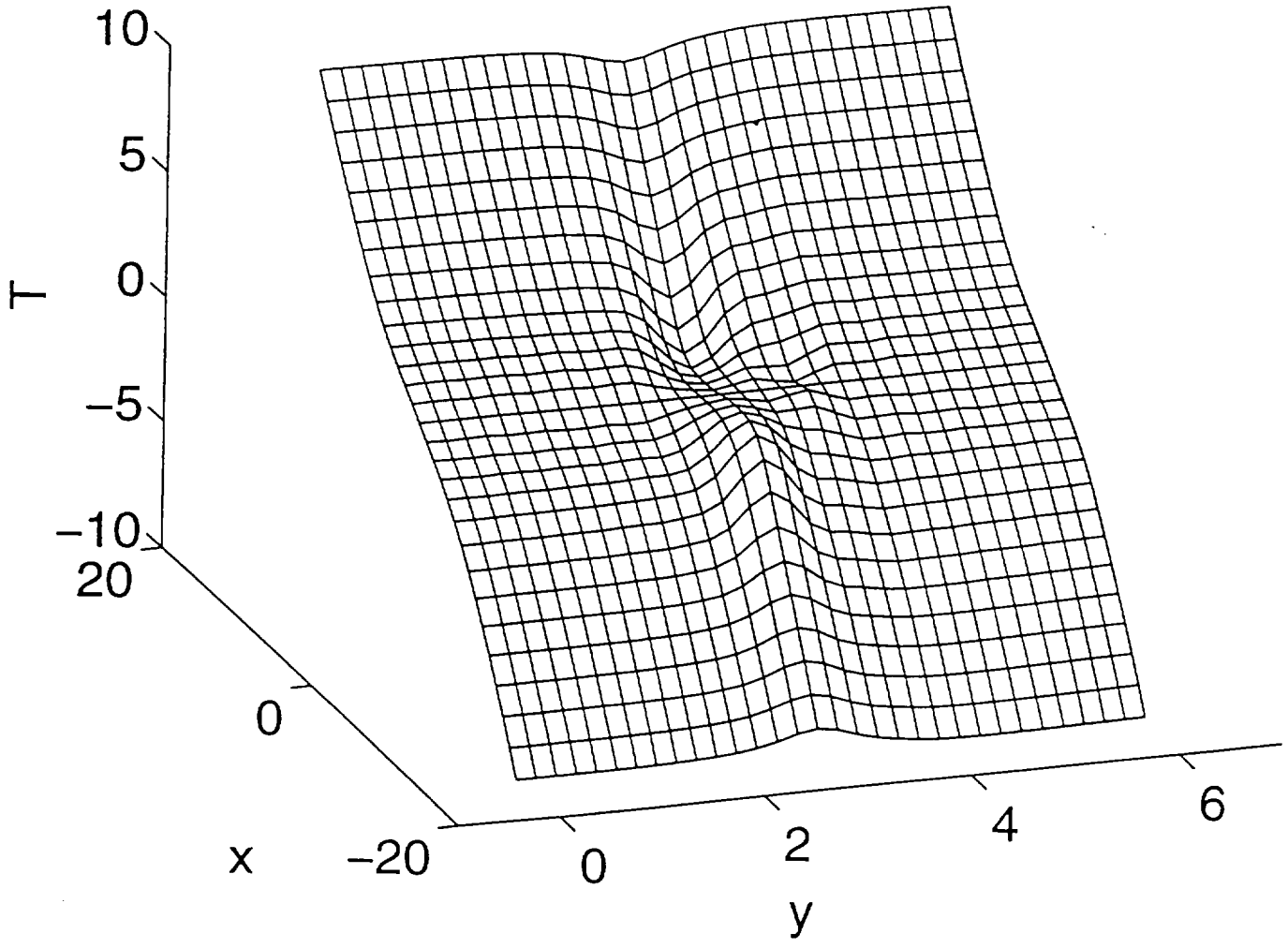

Fig. 36

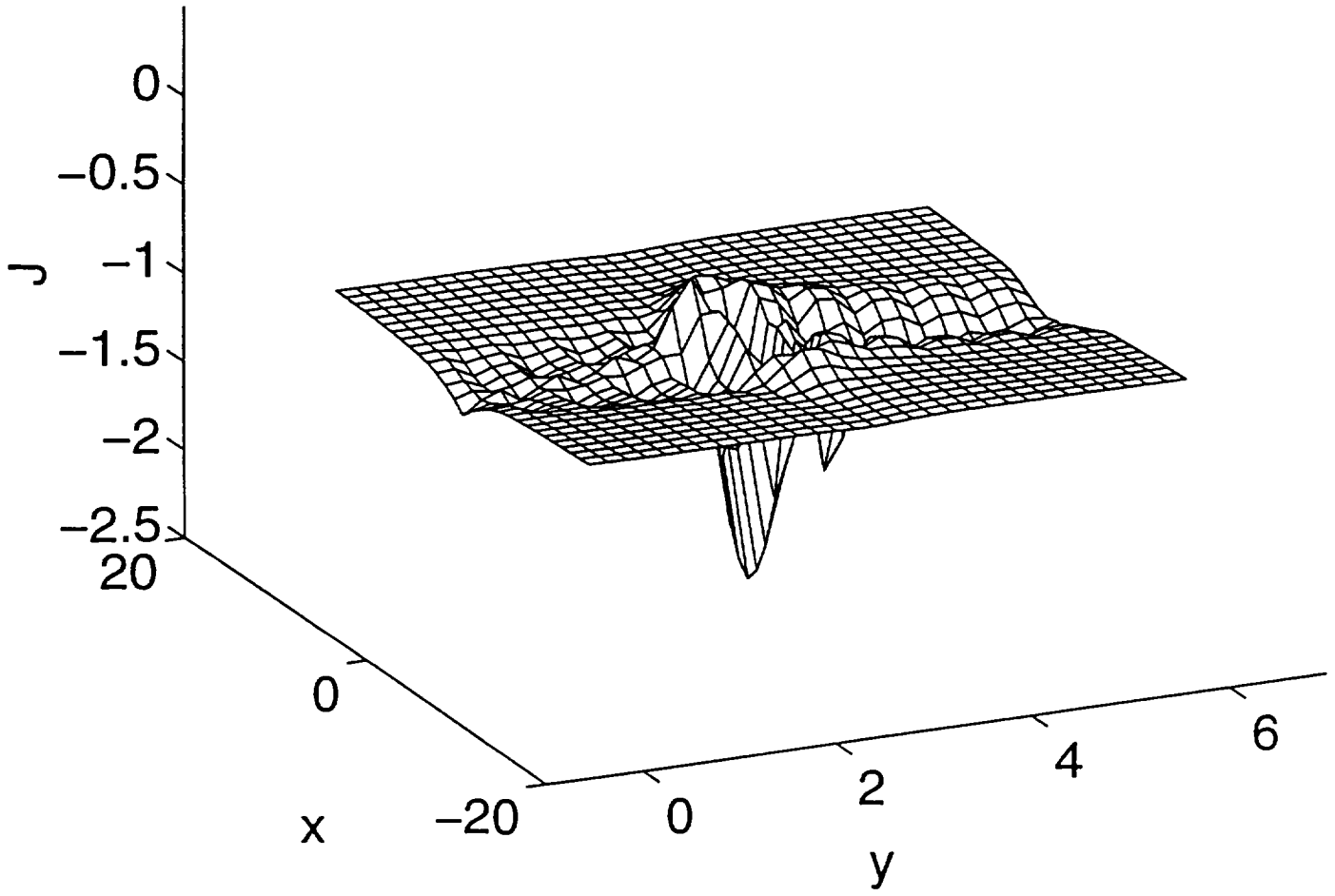

Fig. 4a

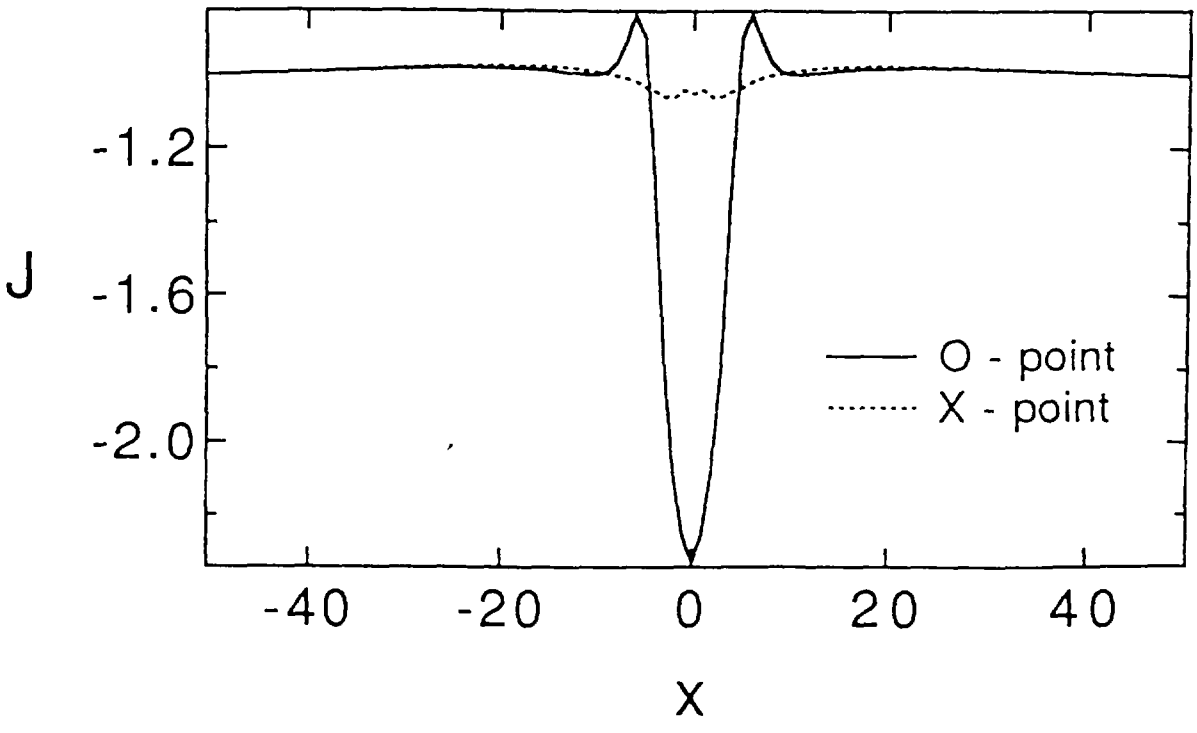

Fig. 4b

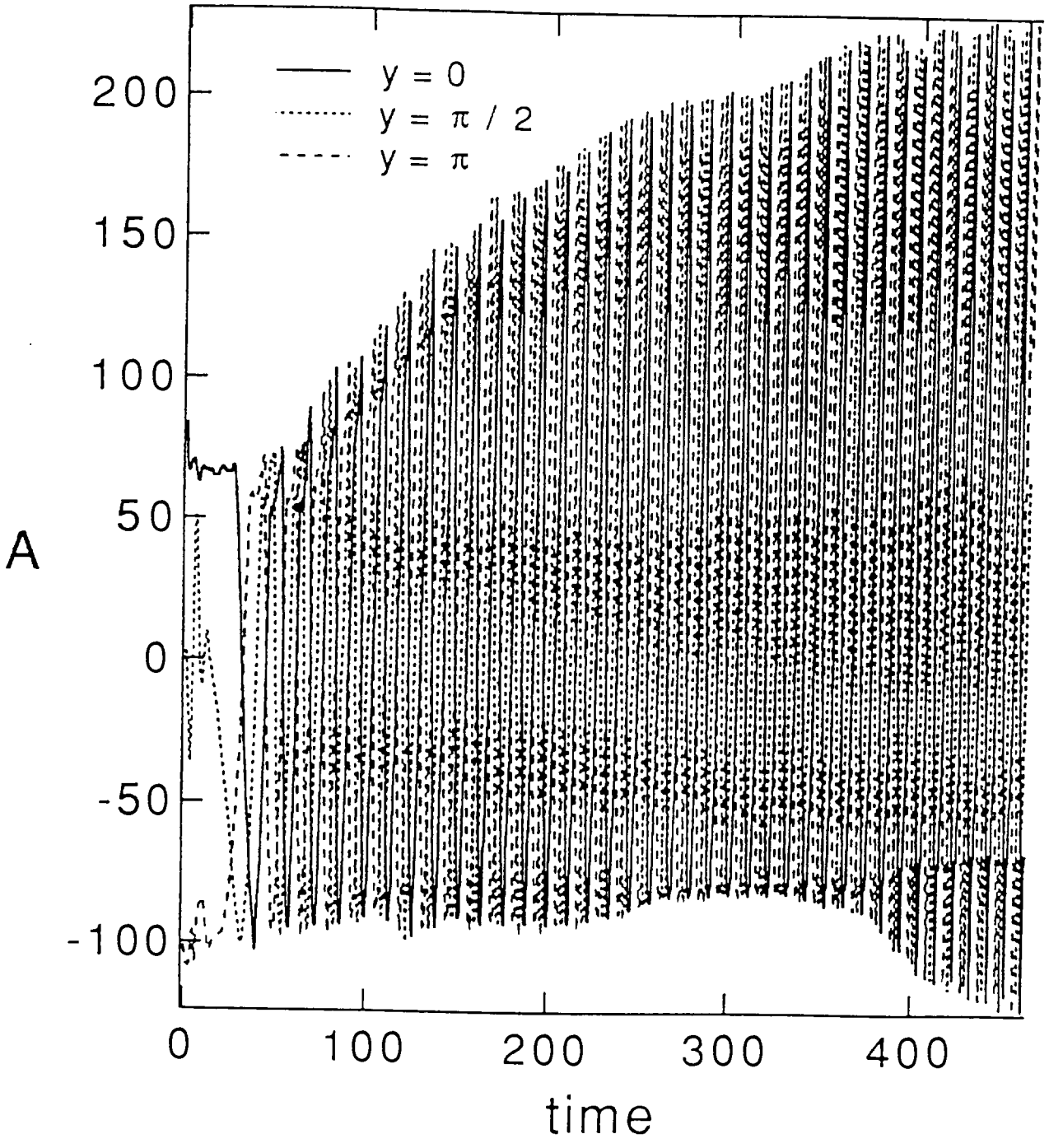

Fig. 5

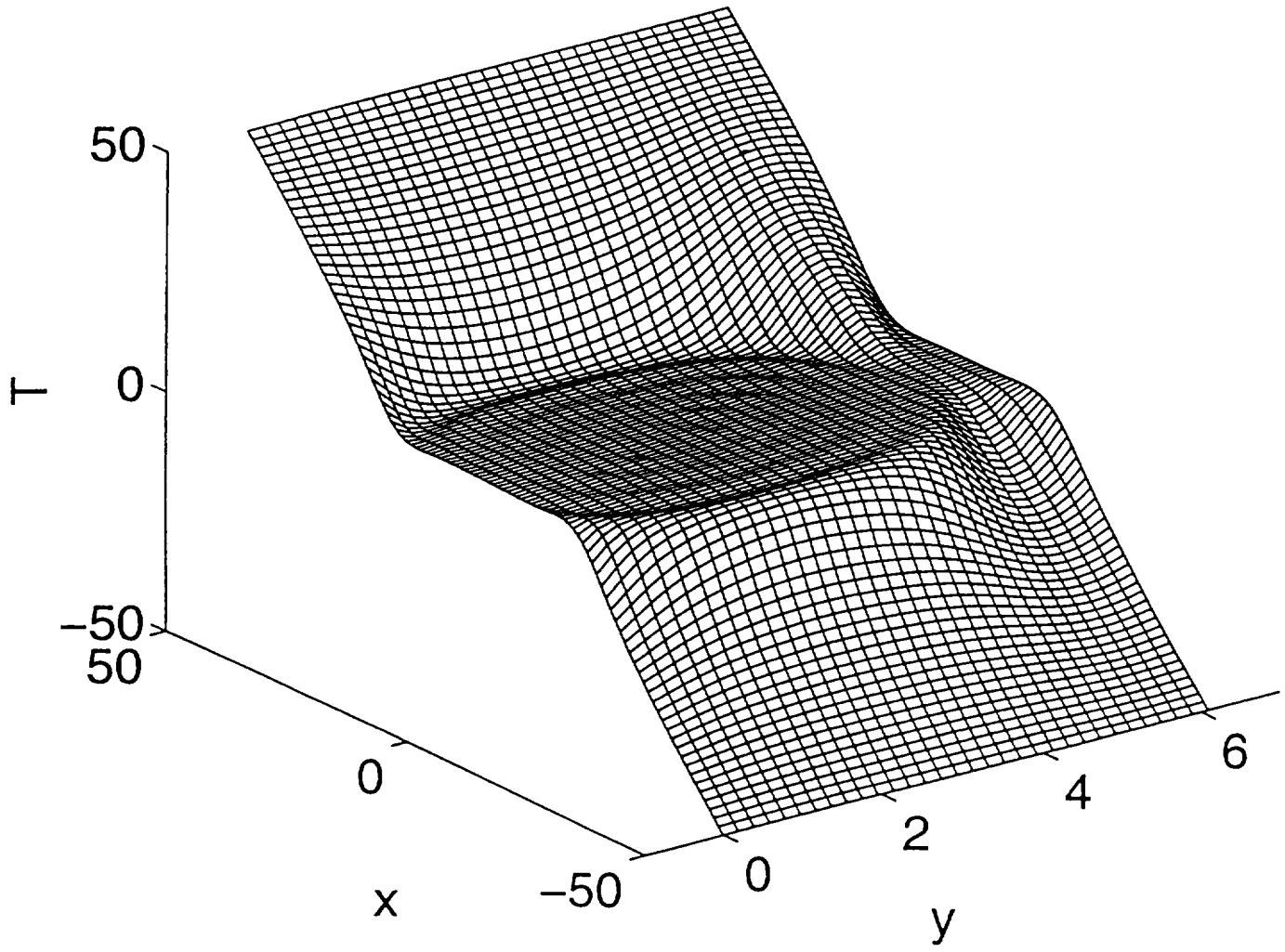

Fig. 6

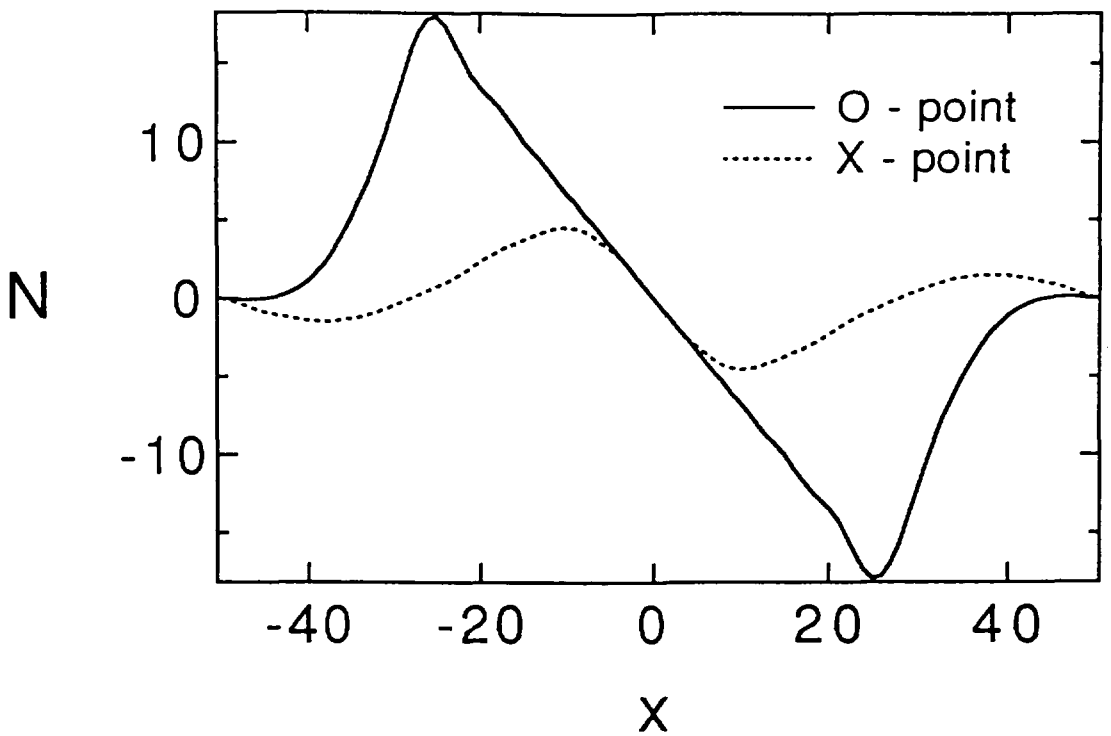

Fig. 7

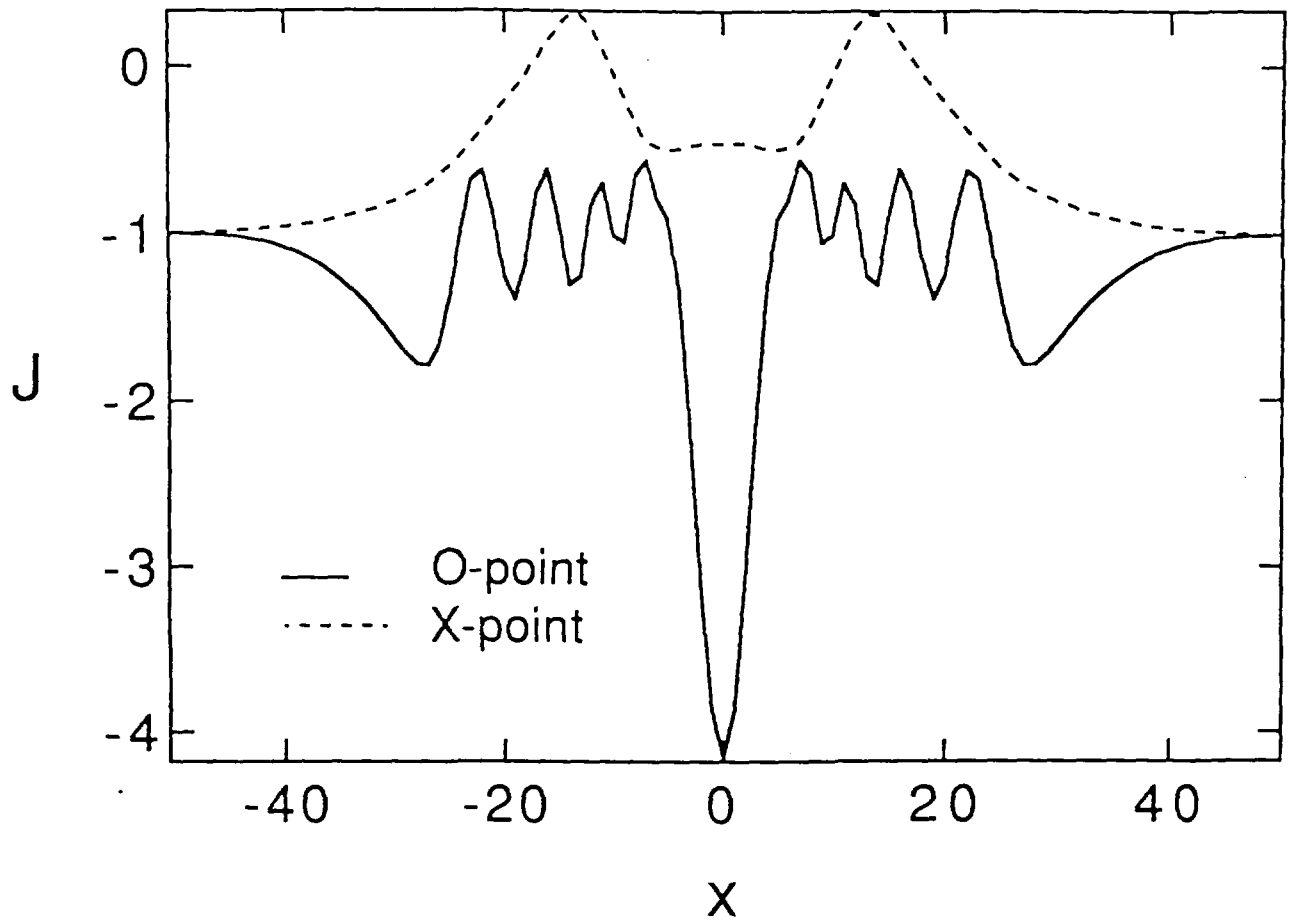

Fig. 8

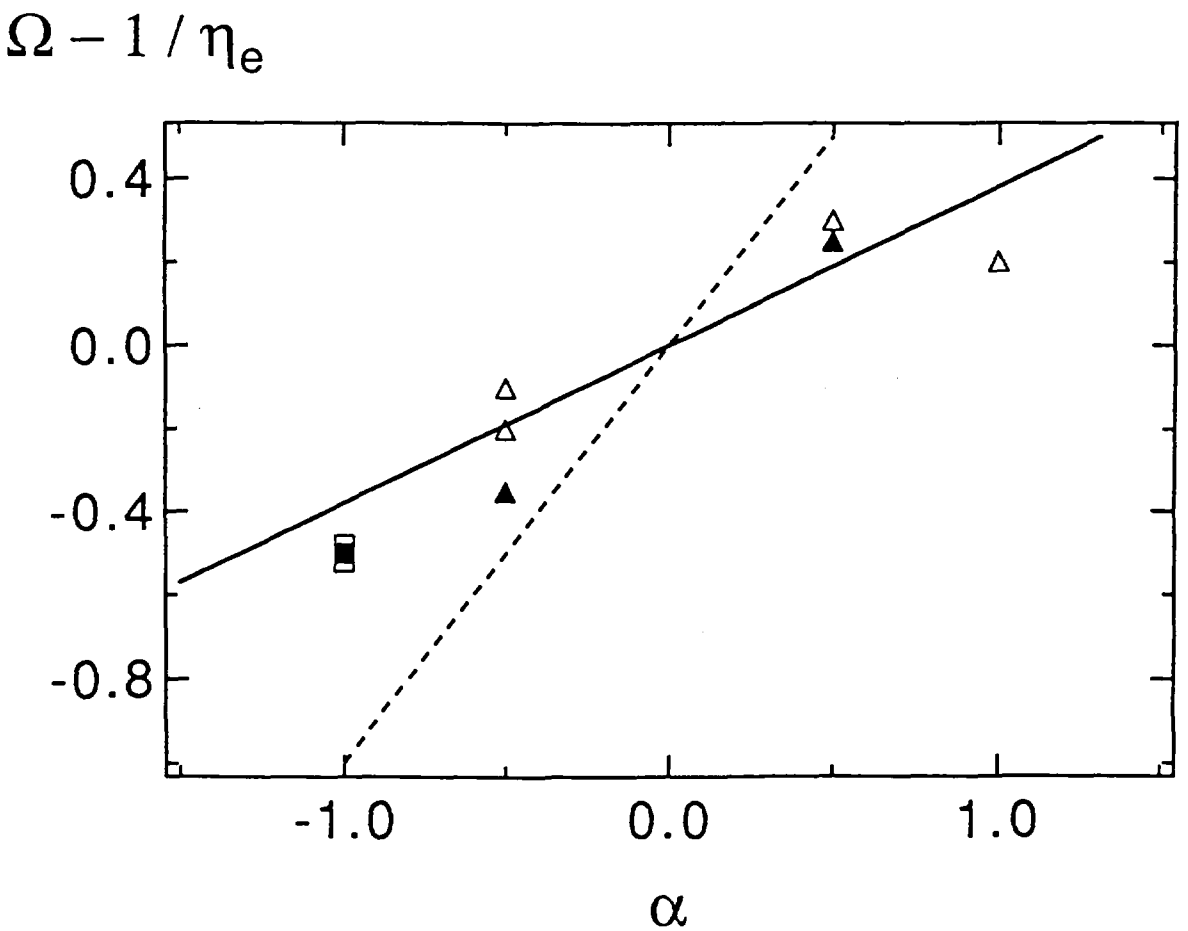

Fig. 9